Neuronal Oscillators in *Aplysia californica* that Demonstrate Weak Coupling *In Vitro*

Amanda J. Preyer and Robert J. Butera*

Laboratory for Neuroengineering, School of Electrical and Computer Engineering, Georgia Institute of Technology, Atlanta, Georgia 30332-0250 USA

(Received 22 April 2005; published 23 September 2005)

Networks of oscillators produce vital activity in diverse natural systems. The dynamics of these networks are frequently studied via computational models that assume weak coupling, yet this assumption has not been experimentally validated. We applied weak stimuli to neuronal oscillators in *Aplysia californica* and deconvolved infinitesimal phase response curves (IPRCs) that describe the phase response of a neuron. We show that these IPRCs reliably predict the phase response for weak stimuli, independent of the stimulus waveform used. These weak stimuli are in the range of normal synaptic activity for these neurons, suggesting that weak coupling is a likely mechanism.

DOI: 10.1103/PhysRevLett.95.138103 PACS numbers: 87.17.Nn, 87.17.Aa, 87.19.La, 89.75.−k

Networks of oscillators are ubiquitous in biological, chemical, and physical systems [1]. Models of these networks are used to understand the dynamics of complex systems, such as entrainment and synchrony [2]. Phase reduction techniques [3–5] have been employed to model many types of these systems, including Josephson junctions [6], semiconductor laser arrays [7], populations of chemical oscillators [8], and neutrino flavor oscillations [9]. These methods are also commonly used to study neural dynamics [10–16]. In these theoretical studies, there is an implicit assumption of weak coupling—that the response model of a phase oscillator is the convolution of an intrinsic response function, often called an infinitesimal phase response curve (IPRC), with the applied stimulus function. Here we experimentally validate the feasibility of weak coupling in a network of neural oscillators. We demonstrate that for sufficiently weak inputs, the measured phase response curves (PRCs) from a neural oscillator scale linearly with stimulus amplitude. We also show that for weak stimuli, nearly identical IPRCs, deconvolved from PRCs, are obtained for different stimuli. This is the first case of an experimentally measured PRC from a neuronal oscillator being provably decomposed into a sensitivity function and an influence function [3].

Phase models describe an oscillation about a limit cycle as

$$\frac{d\theta_i}{dt} = w_i + Z(\theta_i)S(\theta_j), \tag{1}$$

where θ is the phase of an oscillator along its limit cycle, w is the natural frequency of the oscillator, Z describes the oscillator's infinitesimal response (IPRC) as a function of the phase of oscillator i, and S is the stimulus waveform as a function of the phase of another oscillator, j. Analysis of such models typically reduces a network of phase oscillators down to a system of variables representing phase differences, which are solved for the existence of synchronous solutions. These phase reduction methods assume weak coupling between oscillators, and rely upon a mathematical description of the PRC, initially described by Winfree [3] as

$$H(\phi) = \int Z(\psi + \phi)S(\psi)d\psi, \tag{2}$$

where H is the PRC of an oscillator for a given IPRC and stimulus.

For this study, we generated PRCs from neurons in the abdominal ganglia of *Aplysia californica* using different stimulus waveforms. Figure 1(a) contains a block diagram of the experimental setup. Standard sharp electrode intracellular recording techniques were used to stimulate and

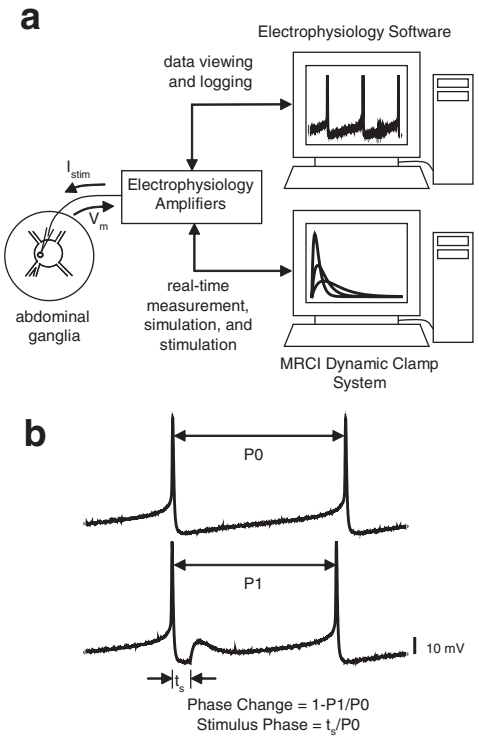

FIG. 1. (a) Block diagram of the experimental setup. (b) Sample voltage traces showing a typical period of the neuronal oscillator and a perturbed period with the stimulus applied at t_s.

record regularly firing neurons in the left lower quadrant of the ganglia. These are tonically firing neurons, which were used in some of the earliest entrainment studies done by Perkel [17]. They spike with periods of 200–500 ms. The firing rate is typically quite regular, with the coefficient of variation of the interspike interval varying from 0.0072 to 0.1549, with a mean of 0.0436. We used a high Mg^{2+}, low Ca^{2+} solution to synaptically isolate the cells within the ganglia.

PRCs are commonly measured experimentally as a way to quantify the behavior of a neuron, without needing to understand the underlying mechanisms [18,19]. A common method for generating PRCs is to stimulate the neuron at different phases throughout its limit cycle and measure the change in period resulting from the stimuli. An example of the procedure is shown in Fig. 1(b). We used the Model Reference Current Injection (MRCI) dynamic clamp system [20,21] to create the stimuli. This setup allowed us to create stimulus currents from alpha-shaped synaptic conductance waveforms, similar to the ones shown on the bottom monitor in Fig. 1(a), with various amplitudes and time constants. The PRC is a plot of the amount of phase change generated by the stimulus as a function of the phase where the stimulus is applied. Some example PRCs are shown in Figs. 2(a) and 2(b). All phases were normalized to the period of the cycle preceding the stimulus.

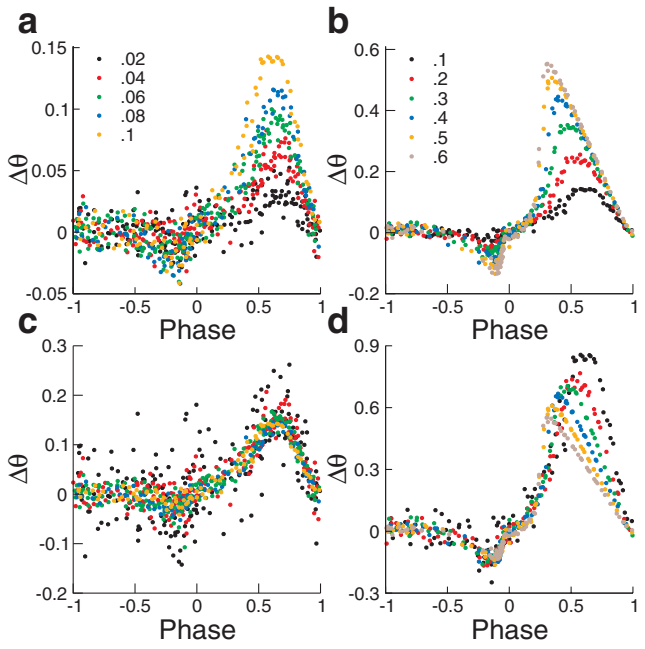

FIG. 2 (color). Weak amplitude stimuli elicit PRCs that scale linearly with amplitude, while large stimuli do not. PRCs were obtained from the same neuron for a wide range of stimulus amplitudes, for $\tau = 10$ ms. Cobalt chloride saline was used to eliminate synaptic input. (a) Weak stimuli PRCs measured for conductances ranging from 0.02 μS–0.1 μS. (b) Strong stimuli PRCs for conductances from 0.1 μS–0.6 μS. (c) Weak stimuli PRCs scaled, point by point, to a conductance of 0.1 μS. (d) Strong stimuli PRCs scaled to a conductance of 0.6 μS.

It has recently been observed that the utility of PRC theory is extended if one considers second order phase resetting [22], i.e., the effects of a stimulus on the cycle after the one in which it is applied. Such extensions seem evident when one considers the effect of nonpulsatile input that arrives towards the end of a cycle. Our analysis incorporates these effects as "negative phase" in our PRCs. Every stimulus is represented by two points on the PRC, a positive phase point describing the effect of the stimulus on the current cycle and a negative phase point representing the effect of the stimulus on the next cycle. Likewise, this view of the PRC, extending from a normalized phase of -1 to 1, is consistent with the facts that our stimuli are applied transiently and that we have assumed a temporal convolution integral, rather than the circular convolution integral in Eq. (2).

To demonstrate that weak coupling is a valid assumption and Eq. (2) is valid, the PRC amplitude should scale linearly with stimulus amplitude, but be shape invariant, and the IPRCs deconvolved from PRCs in response to different stimulus waveforms should be identical. Amplitude scaling was demonstrated by measuring PRCs in response to a wide range of stimulus amplitudes [Figs. 2(a) and 2(b)]. Individual data points of the PRCs were scaled to a common maximal conductance [Figs. 2(c) and 2(d)]. It is evident from these plots that the weak stimuli PRCs scale linearly [Fig. 2(c)], while the strong stimuli PRCs do not [Fig. 2(d)].

The scaling results of Fig. 2 are necessary, but not sufficient, to demonstrate that weak coupling exists. A more convincing demonstration of this phenomenon is to obtain IPRCs for different stimulus shapes. Identical IPRCs signify that the weak coupling integral applies. To do this, PRCs were measured from each neuron for three stimulus waveforms, which differed by the time constant, τ, of the alpha function defining the stimulus; amplitude was scaled such that all stimulus waveforms had a similar integrated conductance. The three PRCs ($\tau = 10$, 20, and 40 ms) with equal integrated conductances will be referred to as a set.

Each PRC in a set was spline fit to remove noise, and the stimulus waveform was deconvolved from the spline fit to obtain the IPRC. Because of the numerical instability of deconvolution, an error minimization algorithm was used to create the IPRCs. We assumed the IPRC was a 10th order polynomial, and found coefficients that minimized the mean squared error (MSE) between the fitted PRC and the IPRC convolved with the corresponding stimulus waveform. Examples of IPRCs for three neurons are shown in Figs. 3(a)–3(c).

For weak coupling to be valid, the IPRCs must be able to accurately reproduce the phase response of a neuron for different stimulus waveform shapes. To test this, each IPRC was convolved with each of the three stimulus wave-

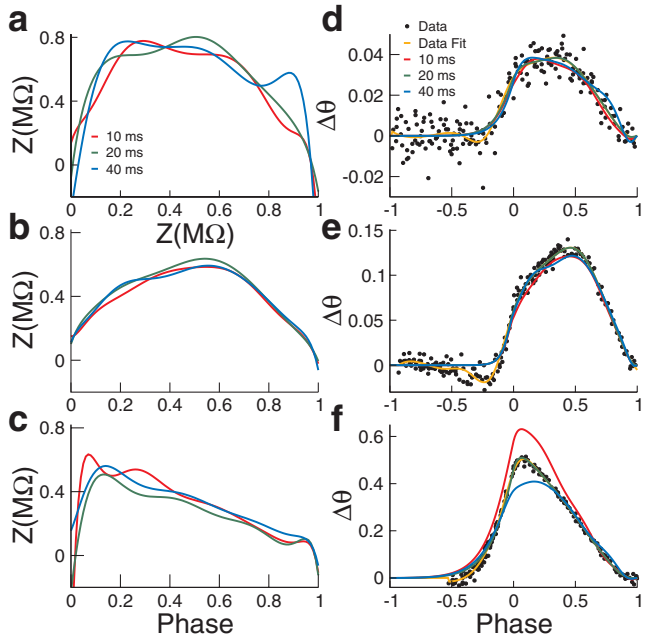

FIG. 3 (color). The IPRCs and reconstructed PRCs for 3 different experiments. (a)–(c) Each show three IPRCs recovered for stimuli with $\tau = 10$, 20, and 40 ms. (d)–(f) The response functions convolved with stimulus waveforms are better able to reproduce PRC data for weak amplitude PRCs. Data points are the measured PRCs in response to stimuli with $\tau = 20$ ms. The orange line is a spline fit to the PRC data points, red, green, and blue lines are the convolution of the IPRCs shown in panels (a)–(c) with the $\tau = 20$ ms stimulus waveform. The rows correspond to different experiments with a set conductance (g) and maximum PRC amplitude of the 10 ms PRC ($\Delta\theta$) of (1) $g = 0.005$ μS, $\Delta\theta = 0.038$; (2) $g = 0.04$ μS, $\Delta\theta = 0.095$; (3) $g = 0.12$ μS, $\Delta\theta = 0.694$.

forms in the set. For example, the 20 ms stimulus waveform was convolved with the 10, 20, and 40 ms IPRCs. The resulting waveforms were compared to the original 20 ms PRCs [Figs. 3(d)–3(f)] and the MSE between the convolved waveform and the spline fit of the experimental PRC was tabulated (Table I). We found for all experiment sets that the MSE was a very good indicator of the quality of the fit of the reconvolved PRC [compare fits in Figs. 3(d)–3(f) with data in Table I].

To compare the quality of fit of the reconvolved PRCs across all experimental sets, the maximum amplitude of the PRC was used as a measure of stimulus strength, in lieu of stimulus amplitude. The use of PRC amplitude accounts for the fact that different neurons have different input impedances. Figure 4 illustrates the MSE as a function of maximal PRC amplitude, for all experimental sets ($n = 36$ sets, from 12 different neurons). At lower PRC amplitudes, the MSE decreases by several orders of magnitude. Thus, the convolution integral reliably reproduces the neuronal response for weak stimulus strengths, but not strong ones. The weak range includes values that are similar to the

TABLE I. MSE results for the three experiments in Fig. 3. The values represent the MSE between the PRC data (τ in rows) and the convolution of the IPRC (τ in columns) and the stimulus waveform (τ in rows). Experiments correspond to a set conductance (g) and maximum PRC amplitude of the 10 ms PRC ($\Delta\theta$) of (a) $g = 0.005$ μS, $\Delta\theta = 0.038$ (b) $g = 0.04$ μS, $\Delta\theta = 0.095$ (c) $g = 0.12$ μS, $\Delta\theta = 0.694$. Numbers in brackets denote powers of 10.

	Stim.	**IPRC**		
Expt.	τ	10	20	40
a	**10**	3.2[−6]	7.7[−6]	1.7[−5]
	20	4.9[−6]	2.4[−6]	7.1[−6]
	40	5.2[−6]	3.3[−6]	1.9[−6]
b	**10**	4.0[−5]	6.1[−5]	5.0[−5]
	20	5.6[−5]	3.4[−5]	4.8[−5]
	40	2.3[−5]	2.7[−5]	1.7[−5]
c	**10**	4.8[−4]	3.6[−6]	9.0[−3]
	20	4.6[−3]	1.6[−4]	1.6[−3]
	40	5.9[−3]	5.5[−4]	5.6[−5]

normal synaptic input seen by these cells. Similar trends in results were obtained when the R^2 metric was used to measure error.

Prior to blocking synaptic activity in these neurons, the typical postsynaptic potential has an amplitude of 2.5 to 15 mV and does not trigger an action potential. We quantified the amplitude of the voltage deflection in response to our stimuli at a stimulus phase of approximately 0.3. Of those stimuli that did not elicit action potentials, 75% produced deflections of 1 to 20 mV, with the remainder producing larger deflections of up to 40 mV. The stimuli that did elicit action potentials correspond to PRC amplitudes of 0.5 or larger in Fig. 4.

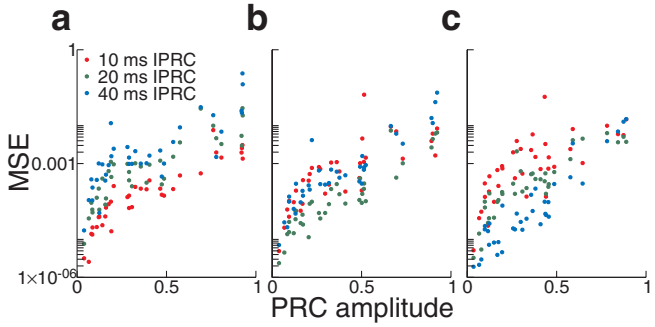

FIG. 4 (color). There is a several order-of-magnitude reduction in MSE for low amplitude PRCs. MSE is plotted as a function of PRC amplitude across all experiments. Red, green, and blue points represent MSEs of reconvolved PRCs for IPRCs in response to $\tau = 10$, 20, or 40 ms stimuli, respectively. IPRCs are convolved with stimulus waveforms and compared to the spline fit PRC data. Panels correspond to stimulus waveforms. (a) $\tau = 10$ ms stimulus. (b) $\tau = 20$ ms stimulus. (c) $\tau = 40$ ms stimulus.

Others have already demonstrated that experimentally obtained PRCs predict situations of entrainment or synchronization [17,22,23]. Their methods did not assume weak coupling, but used a more general type of PRC theory [identical to assuming pulse coupling in Eq. (1)] that relies upon maps of prestimulus to poststimulus phase. Such approaches are limited by the fact that the measured PRC is valid only for the specific stimulus waveform used. Other approaches deconvolve input stimuli from output measures to obtain a ''kernel'' that describes the input-output transformation. This has been applied in several areas of neuroscience to describe stimulus-response experiments. For example, Poliakov *et al.* showed that Wiener kernels could be used to describe how input to a motoneuron was transformed into a time series of output spikes characterized by a peri-stimulus-time histogram [24]. Our method is primarily different from these in that we are studying effects upon a single limit cycle oscillation, while most stimulus-response studies using kernel-based methods typically study longer-term aggregate measures of neural activity that span multiple limit cycles.

Though several groups have measured PRCs from oscillatory excitable cells, and many theorists make the weak coupling assumption in their models, we are aware of only two attempts to deconvolve IPRCs. Galán *et al.* [25] implicitly fit the IPRC as part of a PRC estimation procedure, while Netoff *et al.* [26] use IPRCs to predict the synchronization of coupled oscillators with multiple synaptic inputs. Though these papers implicitly assume weak coupling by calculating IPRCs, neither attempts to systematically validate how consistent the derived IPRCs are with weak coupling assumptions. For example, Netoff *et al.* [26] calculate IPRCs in response to different stimuli. The IPRCs are similar in general shape, but the amplitude and alignment of their deconvolved IPRCs, obtained from the same cell, are noticeably different (Fig. 3 of Netoff *et al.* [26]).

We have successfully demonstrated that there is a range of stimulus strengths where an IPRC can be deconvolved from the PRC of a neuron and the applied stimulus. This function accurately reproduces the phase response of the neuron to other stimulus shapes. The range where this is possible includes coupling strengths comparable to synaptic events seen by these neurons *in vitro*. The results in this Letter are the first to demonstrate that such assumptions may be realistic in specific cases. This evidence supports assumptions made in phase reduction modeling, which requires weak coupling within networks of oscillators to simplify the systems so network behavior can be studied.

This work was supported by the James S. McDonnell Foundation and the National Institutes of Health.

*Electronic address: rbutera@ece.gatech.edu

[1] A. T. Winfree, *The Geometry of Biological Time*, Interdisciplinary Applied Mathematics Vol. 12 (Springer-Verlag, New York, 2001).
[2] L. Glass, Nature (London) **410**, 277 (2001).
[3] A. T. Winfree, J. Theor. Biol. **16**, 15 (1967).
[4] Y. Kuramoto, *Chemical Oscillations, Waves, and Turbulence* (Springer-Verlag, New York, 1984).
[5] S. H. Strogatz, Physica (Amsterdam) **143D**, 1 (2000).
[6] K. Wiesenfeld, P. Colet, and S. H. Strogatz, Phys. Rev. Lett. **76**, 404 (1996).
[7] G. Kozyre, A. G. Vladimirov, and P. Mandel, Phys. Rev. Lett. **85**, 3809 (2000).
[8] I. Z. Kiss, Y. Zhai, and J. L. Hudson, Science **296**, 1676 (2002).
[9] J. Pantaleone, Phys. Rev. D **58**, 073002 (1998).
[10] G. B. Ermentrout and N. Kopell, SIAM J. Appl. Math. **50**, 125 (1990).
[11] D. Hansel, G. Mato, and C. Meunier, Europhys. Lett. **23**, 367 (1993).
[12] C. Van Vreeswijk, L. F. Abbott, and G. B. Ermentrout, J. Comput. Neurosci. **1**, 313 (1994).
[13] D. Hansel, G. Mato, and C. Meunier, Neural Comput. **7**, 307 (1995).
[14] G. B. Ermentrout, Neural Comput. **8**, 979 (1996).
[15] E. Brown, J. Moehlis, and P. Holmes, Neural Comput. **16**, 673 (2004).
[16] B. Pfeuty, G. Mato, D. Golomb, and D. Hansel, Neural Comput. **17**, 633 (2005).
[17] D. H. Perkel, J. H. Schulman, J. P. Segundo, T. H. Bullock, and G. P. Moore, Science **145**, 61 (1964).
[18] A. D. Reyes and E. E. Fetz, J. Neurophysiol. **69**, 1661 (1993).
[19] A. D. Reyes and E. E. Fetz, J. Neurophysiol. **69**, 1673 (1993).
[20] I. Raikov, A. Preyer, and R. J. Butera, J. Neurosci. Methods **132**, 109 (2004).
[21] A. A. Sharp, M. B. Oneil, L. F. Abbott, and E. Marder, Trends Neurosci. **16**, 389 (1993).
[22] S. A. Oprisan, A. A. Prinz, and C. C. Canavier, Biophys. J. **87**, 2283 (2004).
[23] T. I. Netoff, M. I. Banks, A. D. Dorval, C. D. Acker, J. S. Haas, N. Kopell, and J. A. White, J. Neurophysiol. **93**, 1197 (2005).
[24] A. V. Poliakov, R. K. Powers, and M. D. Binder, J. Physiol. **504**, 401 (1997).
[25] R. Galán, G. B. Ermentrout, and N. Urban, Phys. Rev. Lett. **94**, 158101 (2005).
[26] T. I. Netoff, C. D. Acker, J. C. Bettencourt, and J. A. White, J. Comput. Neurosci. **18**, 287 (2005).